Fizika Nizkikh Temperatur, 2003, v. 29, No. 5, p. 577–589

On the orientational relief of the intermolecular potential and the structure of domain walls in fullerite C_{60}

Julia M. Khalack[1,2] and Vadim M. Loktev[1]

[1]*Bogolyubov Institute for Theoretical Physics of the National Academy of Sciences of Ukraine*
14b Metrologichna Str., Kyiv-143, 03143 Ukraine

[2]*Stockholm University, Arrhenius Laboratory, Division of Physical Chemistry*
S-106 91 Stockholm, Sweden
E-mail: julia@physc.su.se; vloktev@bitp.kiev.ua

Received November 29, 2002

A simple planar model for an orientational ordering of threefold molecules on a triangular lattice modeling a close-packed (111) plane of fullerite is considered. The system has 3-sublattice ordered ground state which includes 3 different molecular orientations. There exist 6 kinds of orientational domains, which are related with a permutation or a mirror symmetry. Interdomain walls are found to be rather narrow. The model molecules have two-well orientational potential profiles, which are slightly effected by a presence of a straight domain wall. The reason is a stronger correlation between neighbor molecules in the triangular lattice versus the square lattice previously considered. A considerable reduction (up to one order) of the orientational interwell potential barrier is found in the core regions of essentially two-dimentional potential defects, such as a three-domain boundary or a kink in the domain wall. For ultimately uncorrelated nearest neighbors the height of the interwell barrier can be reduced even by a factor of 10^2.

PACS: **61.48.+c**, 78.30.Na

1. Introduction

The elegant hollow cage structure of the C_{60} fullerene molecule has drawn the close attention of scientists because of its unique icosahedral symmetry I_h. The nearly spherical form of the molecule leads to very unusual physical properties of solid C_{60}, fullerite [1–4]. While at room temperature the molecules can be considered to be perfact spheres, the low-temperature properties of fullerite are determined by the deviation of the molecular geometry from spherical. At these temperatures an orientational molecular ordering takes place, which is a basic issue for understanding the results of recent He-temperature experiments on heat transport [5,6], linear thermal expansion [7,8], and the specific heat [9] of C_{60} fullerite.

The mass centers of the C_{60} molecules in fullerite are arranged in an fcc structure characteristic for close-packed spheres with isotropic interactions between them. At room temperature the molecules are found to be freely rotating. The resulting crystal space group is $Fm\bar{3}m$.

Upon lowering of the temperature, fullerite is undergoes two transitions. At $T \approx 260$ K, it undergoes first-order phase transition, after which the fcc crystal lattice is divided into four simple cubic sublattices. The molecules are now allowed to rotate about one of the 10 molecular threefold axes. The other two of the three rotational degrees of freedom are frozen. Within each of the four sublattices, the allowed molecular rotation axis is fixed along one of the four ([111], $[1\bar{1}\bar{1}]$, $[\bar{1}\,\bar{1}1]$, or $[\bar{1}1\bar{1}]$) threefold cubic axes, so that the crystal space group is $Pa\bar{3}$.

It is worth noting that the truncated icosahedral shape of the C_{60} molecule allows for a more symmetric regular crystal structure with only one sublattice and with the four above-mentioned molecular threefold axes oriented along the threefold crystal axes (usually regarded as the standard molecular orientation). But such a structure is energetically unfavorable for the anisotropic intermolecular interaction. Instead, the observed low-energy structure is obtained by a simultaneous 22° counterclockwise rotation of the C_{60} molecules from the initial standard orientation about their fixed $Pa\bar{3}$ threefold axes.

© Julia M. Khalack and Vadim M. Loktev, 2003

As a result of such a rotation, each C_{60} molecule is oriented in such away that one of the negatively charged double C=C bonds to each of the six neighbor molecules belonging to the same close-packed (111) plane is perpendicular to the molecular rotation axis. To the other six neighbors (belonging to two adjacent (111) planes) the molecule is oriented with the positively charged pentagons (P). Therefore, following a commonly used notation we denote this as the «P orientation». For an ideal structure with all the molecules having a P orientation, every pair of nearest neighbors is characterized by having a pentagon from one molecule opposing a double bond from another molecule.

On the other hand, the potential profile of a fullerene molecule rotating about its fixed threefold axis has an additional metastable minimum* corresponding to an 82° rotation from the standard orientation (and to a 60° rotation from the P orientation). In this minimum, the molecule opposes the neighbor molecules from the same (111) plane with the double bonds, and the molecules from adjacent planes are opposed with hexagons (H orientation**). The energy difference between the P and H minima is about 11 meV (≈ 130 K) and the height of the potential barrier is 235–280 meV (≈ 2700–3200 K) [10,11].

At high enough temperatures, molecules are able to jump between the two energy minima due to the processes of a thermal activation. The average P/H ratio is given by the Boltzmann distribution law. Just below the high-temperature phase transition ($T \approx 260$ K) the fraction of H oriented molecules is close to 0.5, and for $T \approx 90$ K it tends to 0.15 [12].

For temperatures below 90 K the situation changes drastically. The waiting time for a molecule to obtain sufficient energy for a jump between the P and H orientations reaches the order of several days (10^4–10^5 s) or even more. Therefore at some critical temperature (its exact value near 90 K depends slightly on the cooling conditions) the molecules become frozen in their current orientational minima, and a transition to an orientational glassy phase takes place. Below this transition the fraction of H oriented molecules remains practically unchanged and equal to its equilibrium value (about 15%) characteristic for the temperature of the glass transition. In other words, on the average every 7th molecule has the H orientation, and with a very high probability every C_{60} molecule has at least one misoriented neighbor.

While the orientational glass structure is believed to persist down to the lowest temperatures, some of the experimental data obtained at helium temperatures can not be explained in terms of the concept of H oriented molecules alone. For example, the data on heat conductivity [5,6] show a maximum phonon mean free path of about 50 intermolecular spacings, which implies only a 0.02 fraction of scattering («wrong») molecules. Besides, the negative thermal expansion [7,8] and the linear contribution to the specific heat [9,13] of the fullerite samples at helium temperatures are explained in terms of the tunneling (i.e., quantum) transitions of the C_{60} molecules between nearly degenerate orientational minima. Such a possibility was firstly assumed in Ref. 14, where all the molecules in a crystal were assumed to be in tunneling states. However, the paper [13] accurately estimates the tunneling frequency to be about 5.5 K, and the number of tunneling degrees of freedom to be $\sim 4.8 \cdot 10^{-4}$ $(N/60)$, where N is the number of carbon atoms in the crystal. Obviously, the number of a H oriented molecules is much bigger, and the above-mentioned potential barrier between the H and P orientations is too high to provide such a low tunneling frequency. Therefore the defect states other than the simple H oriented molecules should be considered.

One of the possibilities for a realization of the low potential barrier for C_{60} molecule is indicated in our previous paper [15]. Relatively low barrier sites can appear within the orientational domain walls because of the superposition of the mutually compensating potential curves due to interaction with the neighbor

* We do not consider to be distinct the energy-degenerate minima obtained by 120° rotation about the threefold molecular axis.

** Strictly speaking, the term «H (or P) configuration» is more adequate for describing a mutual orientation of two neighboring molecules. Nevertheless, for every chosen pair of neighboring molecules (let us denote them as A and B) with fixed directions of the allowed rotation axes, the mutual orientation depends strongly only on the rotation angle of one molecule (say, A). The other molecule (B) is always (at any angle of its rotation) turned to the first one (A) with a double bond. Therefore, the interaction energy of the pair weakly depends on the rotation angle of the second molecule. As to the molecule A, it is at any rotations always turned to B with a belt of pentagons and hexagons interconnected by single bonds. Thus it is the molecule A of the pair A,B that is responsible for the mutual orientation. Aside from this, upon the rotation of the molecule A from orientation P to orientation H this molecule becomes turned with hexagons (instead of pentagons) to five more its nearest neighbors. At the same time, the energy of its interaction with the other 6 nearest neighbors remains practically unchanged, because the energy depends mainly on the orientation of those latter molecules. For the reasons mentioned above, we follow the common notations and use the letters «P» and «H» to denote the orientation of a single molecule, while keeping in mind those 6 pair orientations for which this molecule rotation angle is crucial.

molecules belonging to different domains. For the case of orientational ordering of hexagons on a square planar lattice considered in [15], the height of the potential barrier in the wall is found to be 5 times less than in the regularly ordered lattice. Such a lowering seems to be insufficient to provide the necessary magnitude of tunneling frequency following from the available experimental data analysis [13].

Meanwhile, most of the results obtained for a square lattice seem to be caused by the incompatibility of the molecular threefold C_3 symmetry axis with the lattice fourfold C_4 symmetry axis. In the case of fullerite, a fullerene molecule has the 4 threefold axes and 3 twofold axes intrinsic to the fcc lattice. Furthermore, the closest-packed (111) plane of the $Pa\bar{3}$ lattice has a hexagonal structure. Six of the 12 nearest neighbor molecules belong to a hexagonal plane, while only 4 of them belong to the same square (001) plane.

Therefore it is interesting and necessary to investigate the main features of orientational ordering for the case of a molecular symmetry identical to that of the lattice. In the present paper we are concerned with the possible orientational domain structures formed by simple flat hexagonal molecules arranged in a (more relevant to a real situation) hexagonal lattice, with both the molecule and the lattice symmetry axes being C_3. The main purpose of this paper is to estimate the intermolecular interaction energy barriers for both the regular close-packed planar structure and for the vicinity of extended orientational defects.

It is a pleasure and a honor for us to dedicate this paper to Prof. Vadim G. Manzhelii a Ukrainian low-temperature experimentalist of world-wide reputation whose contribution to the physics of cryocrystals in general and to the physics of fullerites and fullerides, in particular, is well known and cannot be overestimated.

2. Model

Let us consider a system of flat hexagonal molecules* located at the sites of a rigid hexagonal planar lattice, modeling a (111) plane of the 3D fcc lattice.

Following the empirical potentials used for modeling the intermolecular fullerene interaction (see, for example, Ref. 16 and references therein), we suppose two kinds of negative charges, $-(1 \pm \alpha)$, to be located at the centers of the sides of the hexagon (see, the large and small filled circles in Fig. 1,*a*). These negative charges recall single and double covalent bonds between carbon atoms at the hexagon edge of the truncated icosahedral fullerene molecule. Introduction of the charge parameter α reduces the C_6 hexagonal symmetry down to the C_3 symmetry intrinsic to real C_{60}. The requirement of electrical-neutrality of the model hexagon molecule stipulates the presence of unit positive charges at its vertices (shown with the open circles in Fig. 1,*a*).

For the initial orientation (an analog of the standard orientation in fullerite) the molecules are chosen

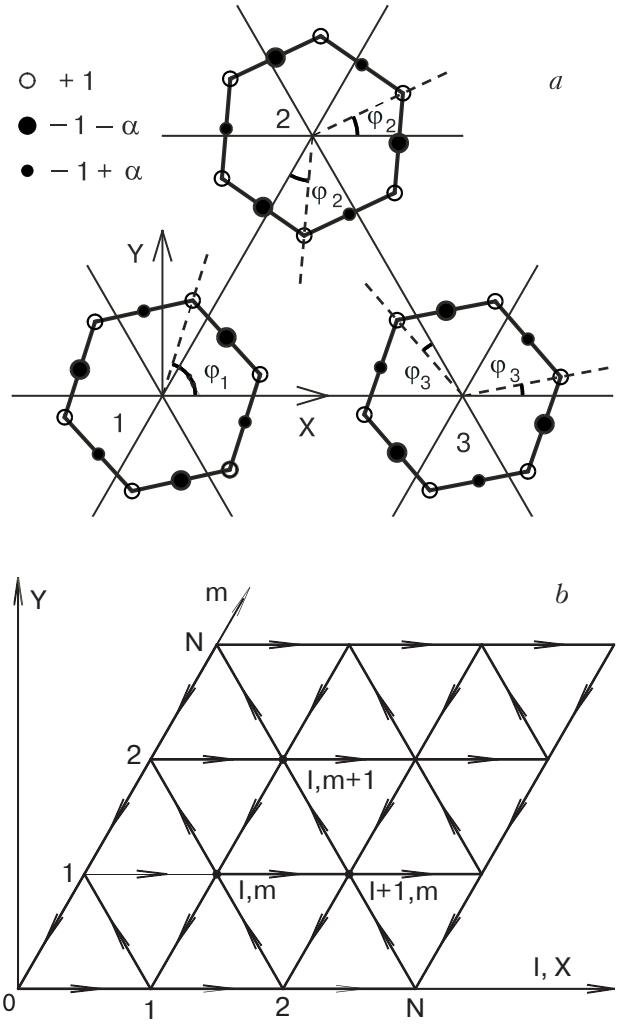

Fig. 1. (*a*) A local geometry of the model molecules on the triangular lattice. Note that molecular rotation angles (shown with the help of dashed lines) can be measured from any of the three lattice directions. (*b*) A geometry of the simulation cell. Arrows give the $1 \to 2$ order of the input parameters for the pair interaction function $W(\varphi_1;\varphi_2)$.

* In some sense, they can be regarded as imitating the C_{60} molecules viewed along the C_3 axis. Strictly speaking, such imitation is realistic only for the fullerene molecules with the fixed C_3 axis perpendicular to the considered (111) plane. The C_{60} molecules belonging to other three $Pa\bar{3}$ sublattices have their fixed threefold axes tilted to this plane.

to be aligned with the positive charges along the lattice directions. The topmost (positive Y direction) negative charge has to be the larger one (see Fig. 1,*a*). The molecular rotation angle φ is measured starting from the positive X direction.

The interaction between two nearest molecules is given by the superposition of the Coulomb interactions between the vertices and bonds of these molecules. The exact form of the resulting interaction function can be found in Ref. 15 (Eqs. (1)–(4)). The interaction is multipolar, so it depends not only on the difference of molecules' rotation angles (as for the case of the spin systems with Heisenberg exchange coupling), but essentially on both the angles. So the energy of interaction of the two neighbor molecules characterized by rotation angles φ_1 and φ_2 has to be written as $W(\varphi_1;\varphi_2)$. The clockwise and counterclockwise rotations have different effects on the interaction:

$$W(\varphi_1;\varphi_2) \neq W(-\varphi_1;\varphi_2) \neq W(\varphi_1;-\varphi_2). \qquad (1)$$

On the other hand, a clockwise rotation of the first molecule is somewhat equivalent to a counterclockwise rotation of the second molecule. Hence, the combination of the lattice mirror symmetry with the molecule mirror symmetry leads to the following symmetry relation for the interaction function:

$$W(\varphi_1;\varphi_2) \neq W(-\varphi_2;-\varphi_1). \qquad (2)$$

Rotating the molecules shown in Fig. 1,*a* by an angle $2\pi/3$ (or $4\pi/3$) about a threefold axis located at the center of the triangle 123, one can find that the pair interaction of the molecules 2,3 (or 3,1) is given by the same function $W(\varphi_2;\varphi_3)$ (or $W(\varphi_3;\varphi_1)$, respectively). The relative displacement (which was vertical or horizontal in the case of the square lattice considered in Ref. 15) of the two molecules does not have to be taken into account, but the order of the angle parameters is essential.

For a simulation of the possible domain structures, we consider a finite parallelepiped-shaped system, the geometry of which is shown in Fig. 1,*b*. It consists of 20×20 hexagonal molecules labeled with the two indexes l and m. Arrows show the order of the interaction function arguments for each pair of hexagons. The system Hamiltonian then reads:

$$H = \sum_{l,m=0}^{N-1}[W(\varphi_{lm};\varphi_{l+1,m}) +$$

$$+ W(\varphi_{l+1,m};\varphi_{l,m+1}) + W(\varphi_{l,m+1};\varphi_{lm})] +$$

$$+ \sum_{l=0}^{N-1} W(\varphi_{lN};\varphi_{l+1,N}) + \sum_{m=0}^{N-1} W(\varphi_{N,m+1};\varphi_{Nm}), \qquad (3)$$

where $N = 19$, and the last two terms are introduced to take into account the edge molecules. For numerical simulations, the charge parameter α is chosen to be 1/3. A hexagon side makes 0.3 of the lattice spacing.

3. Possible ordering types

For the general case of orientational ordering of identical molecules on a planar hexagonal lattice, structures with 1, 3, 4, and 7 sublattices are possible. The one-sublattice structure would correspond to a uniform rotation of all the molecules on a lattice. The three-sublattice structure is characteristic of antiferromagnetic systems (Loktev structure [17]). A close-packed (111) plane of the $Pa\bar{3}$ structure should contain the molecules belonging to four different sublattices. The results of STM imaging of the (111) fullerite surface [18] confirm this fact*. The more complicated case of seven sublattices could be expected for less symmetric molecules.

As to the C_3-symmetric hexagons considered, a rather aesthetic consideration of the threefold site symmetry** implies either the 1- or 3-sublattice case, or a 4-sublattice structure involving three identical rotations. Numerical calculations give for the ground state the three-sublattice structure shown in Fig. 2,*a*. It is interesting to notice that in the 3-sublattice structure the energy minimum corresponds to molecule positions which do not provide the minimum of the pair potential. The molecular rotation angles obtained are ($\alpha = 1/3$):

$$\varphi_1 = 72.37209°;\ \varphi_2 = 25.24477°;\ \varphi_3 = 10.87533°. \qquad (4)$$

Another possible (energy degenerate) ground state can be found with the help of the symmetry relation (2). The corresponding angles are given by

$$\varphi_1' = -\varphi_1;\ \ \varphi_2' = -\varphi_2;\ \ \varphi_3' = -\varphi_3. \qquad (5)$$

* At the beginning of the fullerene era, there were some publications [19,20] reporting an 8-sublattice fcc structure for the low-temperature fullerite. This structure could be obtained by division of each of the four sc $Pa\bar{3}$ sublattices into two fcc sublattices with different (P and H) molecular orientations. However, the 8-sublattice structure has not been confirmed by further investigations. Therefore, we do not consider it here.

** The absence of site symmetry would induce a distortion of the lattice.

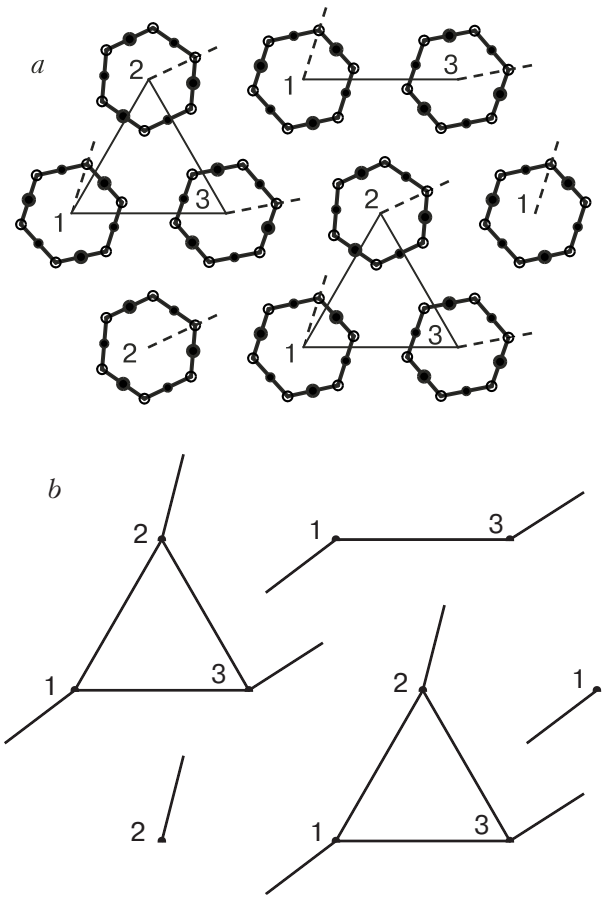

Fig. 2. A ground-state orientational ordering of the hexagonal molecules (*a*), and the same ordering patterned with vectors (*b*).

This ground state is related by mirror symmetry to the state defined by Eq. (4).

The high symmetry of the hexagonal molecules makes it difficult to perceive the ordering pattern presented in Fig. 2,*a*. The more complicated task of finding an orientational defect in this pattern becomes unfeasible. Therefore for the purpose of visualization, we implement a vector representation of hexagonal molecules, shown in Fig. 2,*b*. The vector rotation angle is three times the hexagon rotation angle: $\varphi^{v}_{lm} = 3\varphi^{h}_{lm}$. A vector can be rotated from 0° to 360°. As a result, the difference between sublattices appears more clearly.

Figure 3 shows the change of the interaction of a molecule energy upon a change of its orientation for three molecules belonging to three different sublattices. It is clearly seen that the molecules are not identical. All of them have double-well energy profiles, but the height of the interwell energy barrier varies by a factor of 2. The potential minima of the

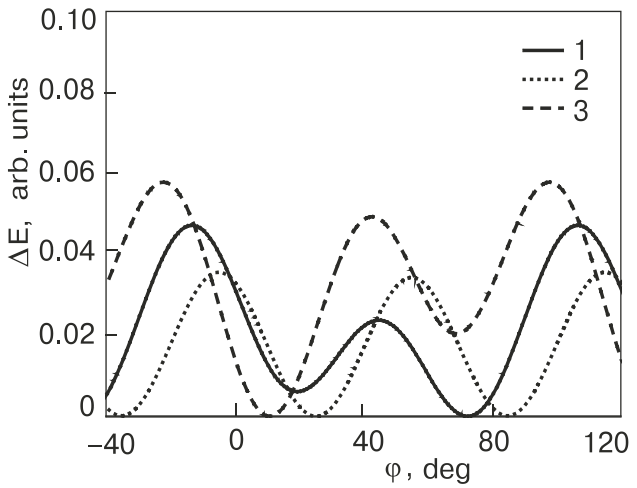

Fig. 3. Orientational potential profiles for regular molecules belonging to three different sublattices.

2nd molecule are almost energy-degenerate, the energy difference being only 1/20 of the barrier height (a situation similar to the case of fullerite).

For comparison, the same potential profiles are shown for the molecules from the edge of the simulated lattice (see Fig. 4). Such molecules keep only 4 of the 6 nearest neighbors (molecules from two different sublattices are missing). As a result, the overall potential profile is lowered by a factor of 6/4. The C_{60} molecule at the fullerite (111) edge surface is missing 3 neighbors from 3 different sublattices. Therefore one could expect a lowering of the orientational barriers by a factor of 12/9*.

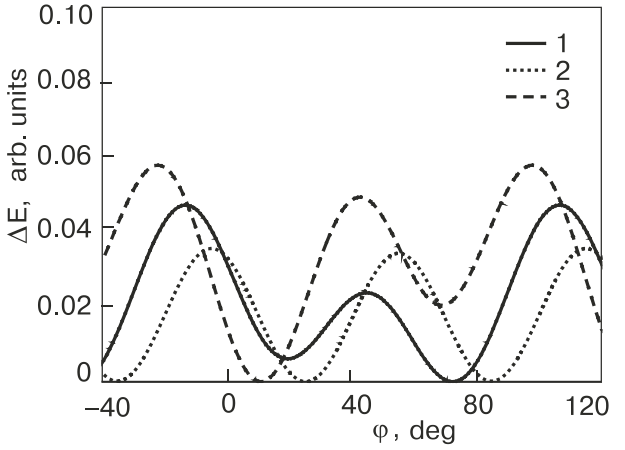

Fig. 4. Orientational potential profiles for the edge molecules belonging to different sublattices.

* Nevertheless, it should be emphasized that the change (or relatively weak lowering) of the intermolecular rotational barriers appears to be too small for all the cases of the regular structure to allow for the orientational tunneling which is necessary for a number of physical phenomena. One has to remember that the mass of the C_{60} fullerene molecule is 720 a.u. This makes a very strong constraint for the height and width of the energy barriers which are able to give the observed probability (or frequencies [13]) of orientational tunneling transitions.

But the real situation is even more complicated. The three-dimensional character of fullerite lattice leads to subdivision of the neighbors of an arbitrary bulk fullerene molecule into only two categories, denoted here as double-bond (for which the molecule is oriented with the double bond), and pentagon (for which the molecule is oriented with the pentagon or hexagon) neighbors. The six double-bond neighbors belong to the (111) plane normal to the molecule fixed C_3 axis. The other six pentagon neighbors, which give a major contribution to the molecular orientational profile, are located in the other (111) planes.

Therefore an edge molecule with a fixed C_3 axis normal to the edge surface is missing three pentagon neighbors, while the molecules with the other three directions of the allowed rotation axis are missing two double-bond and one pentagon neighbor each. As a result, the potential relief of a molecule with a normal rotation axis is shallower than the relief of the other molecules. In this way, the molecules from the four different sublattices which are identical in their rotational properties in the bulk fullerite become non-identical at the edge surface crystal defect due to a loss of symmetry. This non-identity evidently reveals itself in the presence of two additional lower-temperature order–disorder phase transitions reported in [21].

4. Linear orientational defects

A general kind three-sublattice two-dimensional triangular lattice allows for orientational ordering of three different types. Molecular orientations for these ordering types are related to each other by cyclic permutations of the rotation angles φ_i (i = 1, 2, 3; cf. Eq. (4)) for the molecules located at the vertices of a lattice triangle (e.g., the triangle 123 shown by a solid line in Fig. 2). In the case of hexagonal molecules under consideration the existence of the mirror orientational twin defined by Eq. (5) leads to the appearance of three additional ordering types, which are related to the basic permutation ones in mirror symmetry.

As a result, the lattice under discussion allows for the simultaneous existence of orientational domains with 6 different ordering types. A boundary between two domains contains a linear orientational defect (domain wall). Such a defect can involve a permutation (clockwise or counterclockwise) or a mirror transformation (with a center at 3 different lattice sites) of molecular orientations*.

A domain wall of the permutation type is presented in Fig. 5,*a*. The rotation angles of the molecules located at the vertices of a lattice triangle (shown with solid lines) have the values φ_1, φ_2, and φ_3 in the left domain. In the right domain they are equal to φ_2, φ_3, and φ_1, respectively. The domain wall (gray) is relatively narrow. Its width (measured along the horizontal close-packed l direction) is about one period of the 3-sublattice structure. As seen along the close-packed m direction, this defect can be regarded as obtained by the removal of one element from the ideal sequence ...1231231... of molecular orientations. The resulting sequence is ...123|231... .

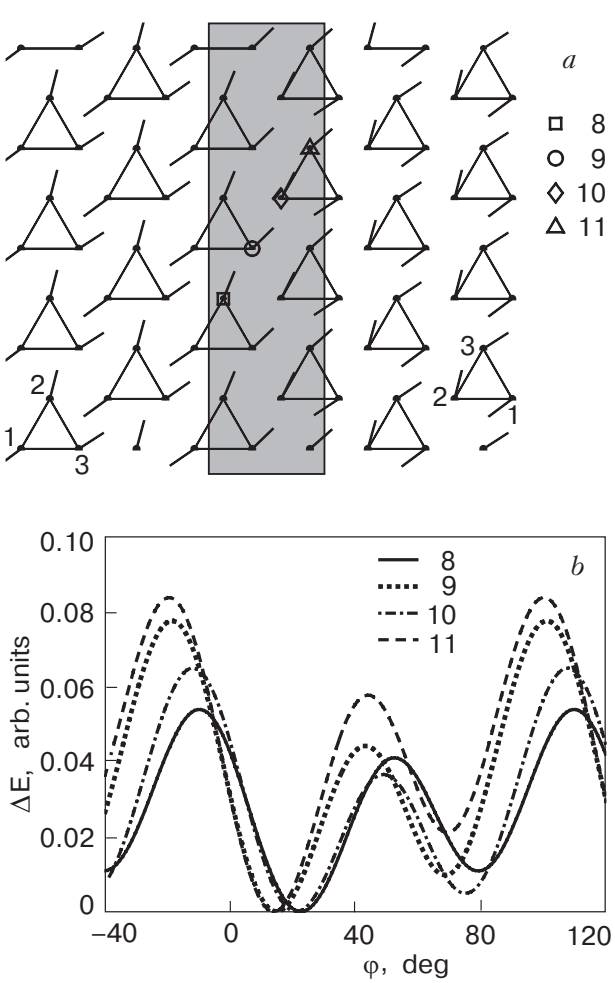

Fig. 5. Permutation domain wall (*a*) perpendicular to a close-packed row, and the orientational potential profiles (*b*) for the four marked molecules identified with the lattice index m (l = 10).

The orientational dependence of the potential energy of the four central molecules from the domain wall is given in Fig. 5,*b*. The molecules are marked in Fig. 5,*a* and labeled with their m index, while l is taken to be 10. Molecules 8 and 10 have orientations of the type 2, and the rotation angles of molecules 9 and 11 are close to φ_3. The potential profiles are quite close in form to the profiles of the regular molecules

* For the case of fullerite, there are 4+4 different ordering types and 3+4 different interdomain boundaries (not related with the symmetry operations).

(shown in Fig. 3), but one of the two potential barriers is lowered for each molecule.

Orientational domain walls of a mirror nature are wider than the permutation ones. Figure 6,*a* gives an example of the mirror domain wall. For this wall, the sequence of molecular orientations in the *m* direction is …123?3′2′1′…, where the question mark stands for a molecule in the mirror plane. This molecule does not fit any regular orientation. Instead, it reflects the mirror symmetry of the wall. Figure 6,*b* clearly shows the orientational potential minimum of the molecule 10 to be located at the rotation angle $\varphi = 60°$. Such an orientation corresponds to aligning one of the mirror planes of the hexagonal molecule with the domain-wall mirror plane.

The mirror symmetry of an orientational defect is also manifested through the symmetry of the potential curves of other molecules. The potential profiles of molecules 9 and 11 (orientations 3 and 3′) and 8 and 12 (orientations 2 and 2′) are related through $\Delta E_9(\varphi) = \Delta E_{11}(-\varphi)$ and $\Delta E_8(\varphi) = \Delta E_{12}(-\varphi)$, respectively.

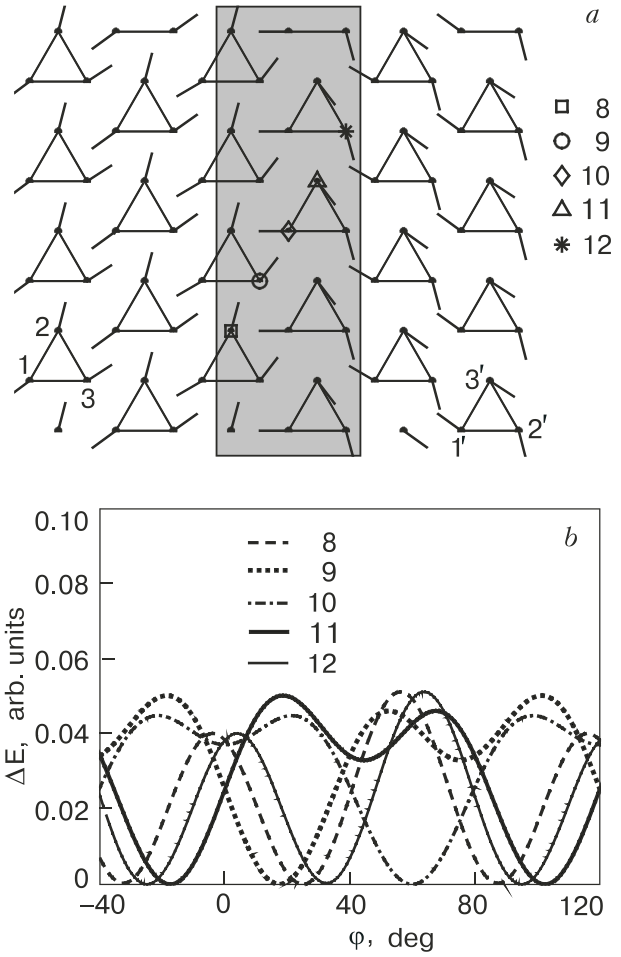

Fig. 6. Mirror domain wall (*a*) perpendicular to a close-packed row, and the potential profiles (*b*) for the five marked molecules with $l = 10$ and with the indicated *m* value.

In the vector pattern of Fig. 6,*a*, this symmetry is given with the clockwise–counterclockwise vector rotations on the two different sides of the wall. Since the rotation angles are measured form the *X* direction, the vectors representing rotation of molecules 9 and 11 (8 and 12) are related by a mirror plane parallel to the *X* direction.

The effect of the domain wall on the potential relief of molecules 8 and 12 (orientations 2 and 2′) is found to consist in a slight lowering of one of the two barriers. For molecules 9 and 11 (orientations 3 and 3′), close to the center of the domain wall, both the potential barriers are lowered considerably. But the position and the relative height of the secondary minimum are unchanged, resulting in the shallow character of this minimum seen in Fig. 6,*b*.

The domain walls given in Figs. 5, 6 have their directions parallel to one of the sublattice period vectors, and perpendicular to one of the close-packed molecular row directions. At the same time, there is a possibility for a domain wall to lie along the close-packed molecular rows. An example of a permutation domain wall of this kind is presented in Fig. 7,*a*. The relationship between the left and right domains here is the same as in Fig. 5, but the location of the domain wall line is different. As a result, the molecular orientation sequence along the *m*th molecular row can now read …231|312… ($l = 8$), …312|123… ($l = 9$), or …123|231… ($l = 10$). Therefore, the central part of the domain wall contains molecules with 6 different potential profiles (orientations 1, 2, and 3 from the left domain, and orientations 3, 1, 2 from the right domain). The three potential profiles with the lowest energy barriers are shown in Fig. 7,*b*. It is noteworthy that here we gain a low barrier profile with almost energy-degenerate minima (see dotted curve).

A domain wall of a mirror nature parallel to a close-packed molecular row has the more complicated structure shown in Fig. 8,*a*. It is again wider than the permutation wall, so that the molecules from *three* close-packed rows have substantially corrupted orientational potential relief. As a result, the number of intra-wall molecules with different orientational profiles increases up to 9, opposed to 6 different profiles for a permutation wall. Furthermore, the direction of the domain wall does not coincide with the lattice mirror plane, so there is no mirror symmetry in the pattern of Fig. 8,*a*, and, accordingly, no symmerty relations for the potential curves (cf. the mirror symmetry of the potential profiles shown in Fig. 6,*b* for a domain wall perpendicular to a close-packed molecular row). In Fig. 8,*b* we give the orientational potential profiles for the three molecules with the lowest interwell energy barriers. It is seen that there exists a

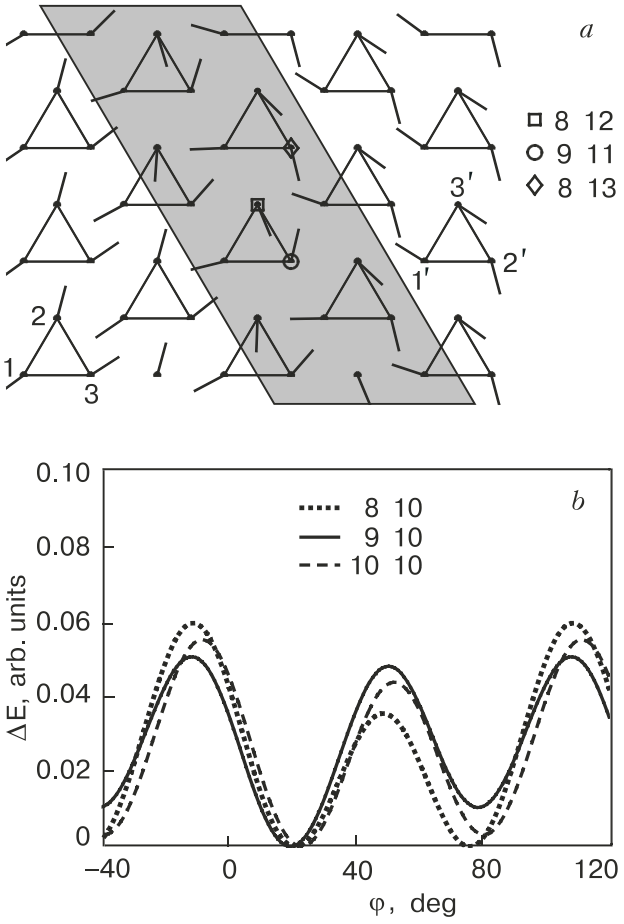

Fig. 7. Permutation domain wall parallel to a close-packed row (*a*), and the orientational potential profiles (*b*) for the marked molecules with the given lattice indices *l* and *m*.

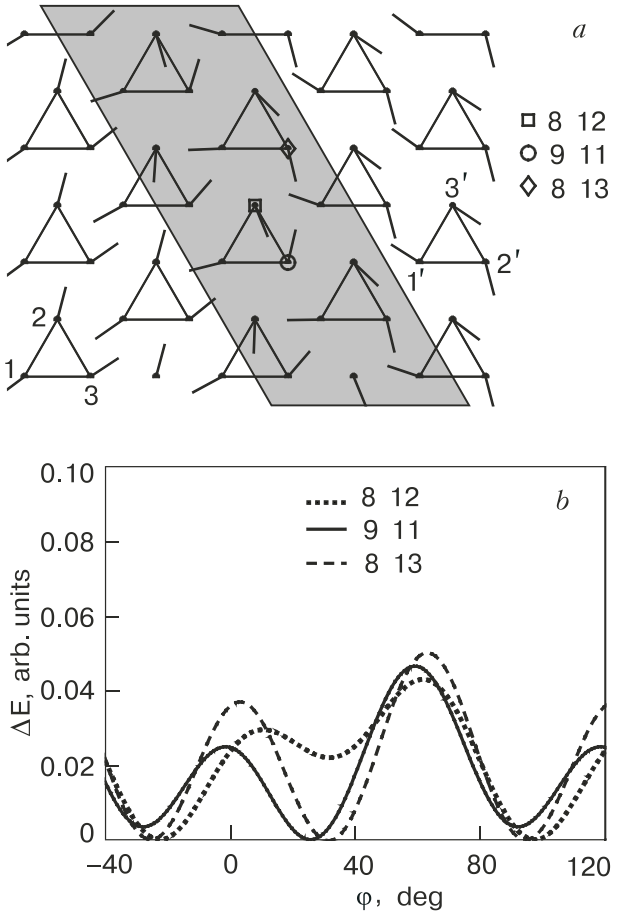

Fig. 8. Mirror domain wall parallel to a close-packed row (*a*), and the potential profiles (*b*) for the marked molecules (the lattice indices *l* and *m* are indicated).

molecule (o) for which the interwell barrier is about 1.4 times lower than the lowest of the interwell barriers of the regular molecules. The molecule is situated at the center of the domain wall and marked with a circle. The corresponding potential profile is plotted by the solid curve in Fig. 8,*b*. The obtained reduction of the orientational interwell barrier is caused by a lower correlation between the nearest-neighbor molecules (every molecule within the considered wall has neighbors of six different orientations).

5. Two-dimensional defects

The results on the modeling of the straight domain walls in the system considered show that the molecules with the shallowest potential profile tend to appear at sites with the reduced correlation between the orientations of the neighbor molecules. For the straight walls this condition is met at the boundary of two domains with different sets of equilibrium molecular orientations (mirror domain walls).

Then it is straightforward to continue the search for the shallow-potential molecules in the core regions of essentially two-dimensional orientational defects. One of such promising two-dimensional defect is a meeting point of three different domains. Molecules at the center of this defect should have three pairs of neighbors belonging to three different domains, so one could expect an additional decrease of the interwell barriers in comparison to the two-domain boundary case.

The results of numerical calculations indeed show a further reduction of the interwell potential barriers at the boundary of three orientational domains. The most effective reduction is found to take place in the presence of mirror boundaries.

Figure 9,*a* shows an example of an orientational defect formed at the intersection of three domain walls perpendicular to molecular rows. The left (narrow) domain wall is of a permutation type, while the other two (the bottom one and the right one) have a mirror nature and are much wider. The right domain wall incorporates a kink in order to minimize the surface spanned by the defect. The molecules with the lowest interwell barriers are marked.

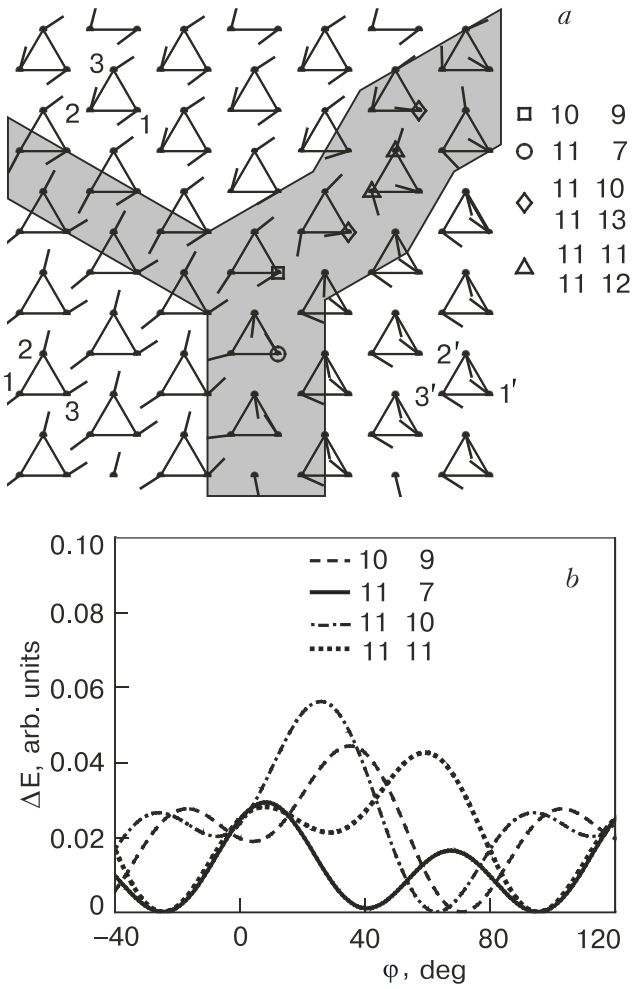

Fig. 9. Structure of orientational defect (*a*) formed at the boundary of three orientational domains, and the potential profiles (*b*) for some chosen molecules in the defect core region. Pairs of molecules marked with the same sign (△ or ◇) have symmetry-related potential profiles, so only one of the profiles is given for each pair. The molecules are labeled by the indices *l* and *m*.

As we have said no significant potential barrier reduction has been observed for straight domain walls perpendicular to close-packed molecular rows. Therefore the marked molecules can be seen only at the crossing of the three walls. The corresponding orientational potential profiles are plotted in Fig. 9,*b*.

It is surprising that the potential profile with the least energy barrier belongs not to the molecule □ situated at the very center of the defect (potential curve plotted with a dashed line) with totally different orientations of all the 6 nearest neighbors, but to the molecule located at the beginning of the bottom domain wall (○, solid line). For the last molecule the orientations of the nearest neighbors differ only slightly from that in the straight wall, but the interwell potential barrier is 2.3 times lower than the lowest regular molecule barrier.

The other four molecules that are marked in Fig. 9,*a* are located within the center of the kink in the right domain wall. At a closer look, one can find a kind of symmetry center at the middle of the line between the molecules marked with △. The exact symmetry is as follows: if the centers of two molecules are related by inversion symmetry, these molecules have rotation angles which are equal in absolute value, but opposite sign. Therefore the two molecules marked with △ (as well as the two molecules marked with ◇) have the same orientational dependence of intermolecular interaction potential, the only difference being in the clockwise or counterclockwise direction of molecular rotation. This can be compared to the symmetry of the potential curves in Fig. 6,*b*, but there is no mirror plane in the present case. To avoid having a very complicated picture, only one of the two symmetry-related curves is shown in Fig. 9,*b* for each pair of molecules. Both the dotted and the dash-dotted curves have an interwell energy barrier which is less than the lowest energy barrier characteristic for regular molecules. This means that at the center of the kink in a domain wall (also a two-dimensional defect) the molecules have ill-correlated nearest neighbors. Therefore the case of a kinked domain wall has to be investigated more thoroughly.

Figure 10,*a* shows the structure of the kink that contains the molecule with the lowest height of the orientational interwell barrier obtained in our simulations. This molecule (in fact, two molecules, since the kink has a center of symmetry of the kind described above) is located at the very center of the kink, and the corresponding potential curve is shown in Fig. 10,*b* by a solid line. The height of the interwell potential barrier is 5 times less than for the case of regular molecules.

6. Totally uncorrelated neighborhood configuration

The three-dimensional defect structure of the real fullerite can be even more complicated. As a result, some molecule can have neighbors whose orientations are fixed by different elements of the defect network. In the framework of our simple two-dimensional model such a neighborhood would be totally uncorrelated, and the height of the interwell barriers could be further lowered. Therefore it is interesting to know the minimum possible height of the molecule interwell potential barrier for an arbitrary orientational configuration of its neighbor molecules.

For this purpose, let us consider a system of 7 hexagonal molecules located at the sites of hexagonal lattice, so that one central molecule has 6 nearest neighbors. The rotation angles of the outer molecules

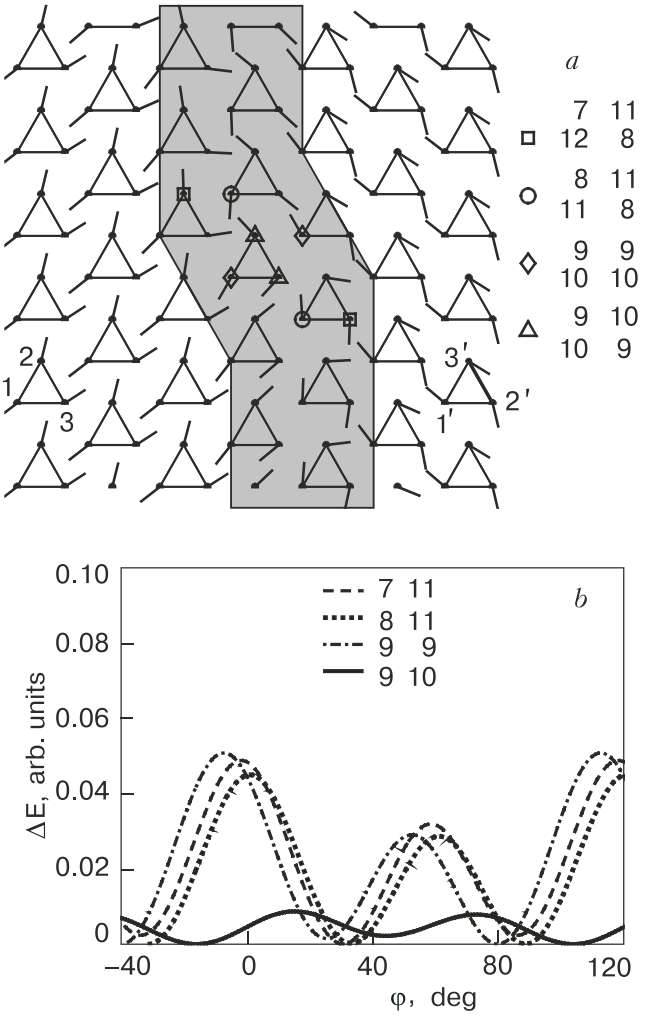

Fig. 10. The structure of a kink in a mirror domain wall (*a*), and the orientational potential profiles (*b*) for the marked molecules. Only one potential curve is given for every pair of symmetry-related molecules which are marked with identical signs. The indices *l* and *m* are indicated.

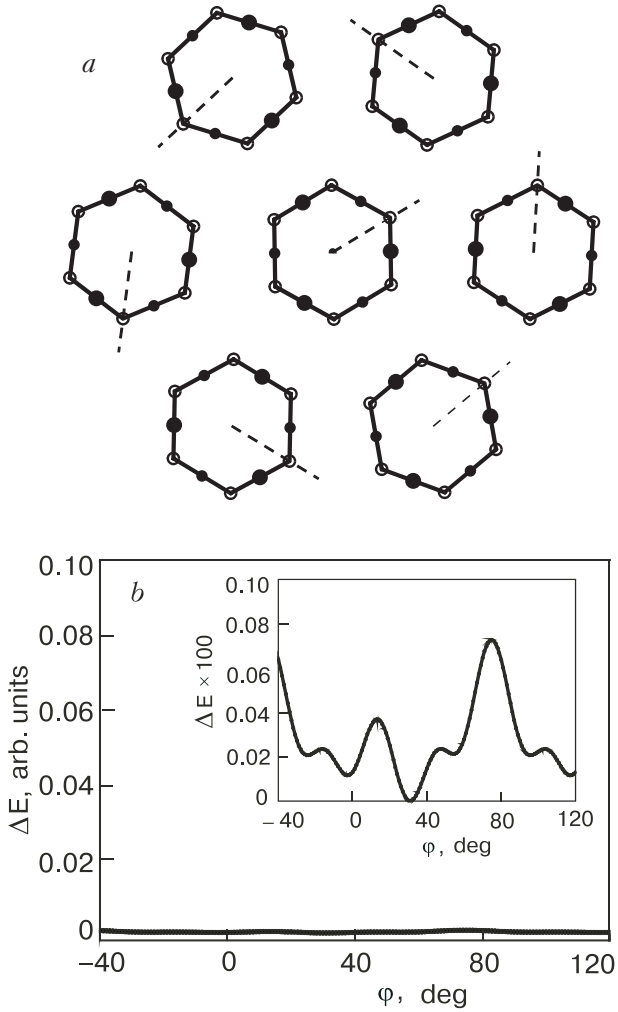

Fig. 11. A molecular configuration with nearly symmetric orientations of the outer molecules (*a*) and the corresponding shallow potential profile of the central molecule (*b*). The inset in the bottom panel shows a magnified potential curve.

are fixed to be equal to 6 random numbers between 0° and 120°, and then the orientational potential profile of the central molecule is calculated. Configurations with the shallowest potential profiles obtained in the course of about 10^6 different realizations of the random neighborhood configuration are shown in Figs. 11, 12, and 13.

Figure 11 gives an example of a molecular configuration with interwell potential barriers of a central molecule reduced by two orders of magnitude with respect to the case of the totally orientationally ordered lattice. This configuration is nearly symmetric (the outer molecules have rotation angles of about ± 30°). The central molecule has a four-well orientational potential profile with the main minimum located close to 30°. One could expect that a completely symmetric configuration might have an even shallower potential profile of the central molecule, because of the increase of the interaction energy at the minima of the potential. Contrary to the expectations, the exactly symmetric configuration (not shown) has an order of magnitude higher interwell barriers than the one shown in Fig. 11. Thus, interwell barriers prove to be extremely sensitive to even very smal rotations of the molecules.

The case of the molecular configuration with a two-well orientational profile of the central molecule is presented in Fig. 12. If one does not take into account the difference between the values of the negative charges, this configuration seems to be close to having a mirror symmetry. It is probably this difference that leads to the increase of the interaction energy at the potential minima.

The molecular configuration with the lowest obtained interwell potential barrier of the central molecule (shown in Fig. 13) has no symmetry at all. The

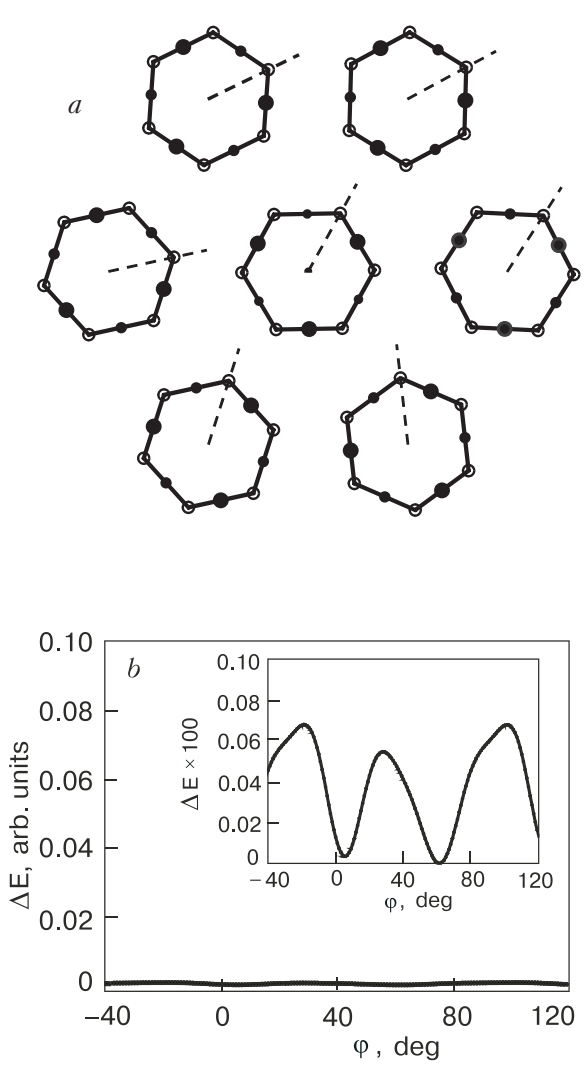

Fig. 12. The same as in Fig. 11: Another nearly symmetric configuration with a two-well potential profile.

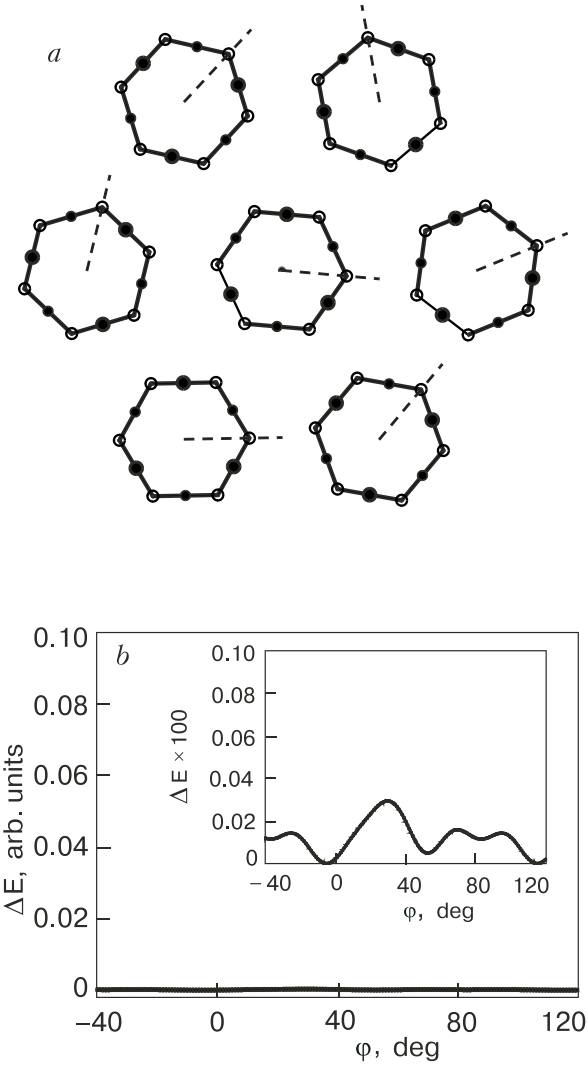

Fig. 13. The same as in Fig. 11: Nonsymmetryc configuration with the lowest interwell barriers found.

orientational profile has three minima of different depth, and the lowest interwell barrier is about 200 times lower than the corresponding lowest barrier in the regularly ordered lattice.

Also it should be noted that the molecules of the regularly ordered lattice (namely, the molecules with the φ_1 orientation, see Fig. 3) have the neighborhood configuration with the highest possible interwell potential barrier. While minimizing the overall interaction energy, this configuration also minimizes the interaction energy at the minimum of the one molecule potential, and deepens this minimum.

7. Discussion

The simple planar model considered recovers some of the features of the fullerite lattice. First of all, it predicts a multi-sublattice structure for a system which would be arranged in a more symmetric 1-sublattice manner in the absence of anisotropic intermolecular interactions.

Then, the model involves lowering of the orientation potential relief of the molecule at the crystal surface. This can be compared favorably to the absence of H-oriented molecules in the STM image of the fullerite surface [18]. Futhermore, at a closer look this image shows a slight difference in orientations of the fullerite molecules belonging to the three sublattices for which the molecular C_3 rotation axes are not perpendicular to the surface. This difference is due to a competition of the two-dimensional character of a surface (with probably another subdivision into sublattices) with the bulk equilibrium orientations of the molecules below the surface molecular layer.

The rather narrow character of the domain walls in the high-symmetry system considered is rather natural for a system with only one kind of

interaction involved*. It agrees well with the very sharp character of the domain wall observed in a two-dimensional monolayer of C_{60} fullerene molecules [22]. This wall contains also a very sharp kink, which is a kind of essentially two-dimensional defect that can incorporate molecules with low orientational interwell barriers.

The sharp character of the observed kink implies the possibility of existence of strongly localized orientational defects also in the bulk of the three-dimensional fullerite. Some of these strongly localized defects with necessarily uncorrelated orientations of the neighbor molecules' orientations should involve molecules with an orientational potential which is sufficiently shallow to give a reasonable frequency of tunneling transitions. As to the rather high C_{60} molecule mass, the recent molecular dynamics simulations of dislocation-kink tunneling [23] in Ag show an efficient of tunneling of complex heavy objects under certain conditions.

The idea of explaining negative thermal expansion of solids by the double-well tunneling statistics was suggested by Freiman in 1983 for the case of solid methane [24]. In the range of temperatures where the conventional phonon mechanism does not work the thermal expansion is established as a result of the competition of two factors. The first factor is a lattice contraction due to the process of populating the tunnel states with an increase of temperature. Shrinking the distances between molecules increases the height of the orientational interwell barriers, which leads to a decrease of the tunneling energy splitting and, as a result, to a decrease of the system free energy. The contraction of the lattice is stabilized by an increase of the elastic part of the free energy for every fixed value of crystal temperature.

Since the population of tunnel states has a very strong exponential temperature dependence, the thermal expansion resulting from the competition of the two factors is always negative. At $T \approx 0$ K it is practically absent (no molecules on excited tunnel levels). With an increase of temperature the population of the excited state grows, and therefore the lattice is contracted. But at $T > \Delta$, where Δ is the tunnel state energy splitting, both the ground and the excited states become almost equally populated, so that the effect becomes much less pronounced. This means that there should exist a maximum in the magnitude of the negative thermal expansion coefficient.

With a simple differentiation of expression (6) of Ref. 24 one can find that this maximum takes place at the temperature $T_{\max}$ satisfying the equation

$$\frac{2T_{\max}}{\Delta} = \tanh\left(\frac{\Delta}{2T_{\max}} + \frac{1}{2}\ln\frac{f_1}{f_2}\right),$$

where f_1 and f_2 are the degeneracies of the ground and excited states, respectively. It is easy to see that $T_{\max} < \Delta/2$ holds for any ratio f_1/f_2.

Therefore the tunneling energy splitting in fullerite can be estimated from the $T_{\max}$ position in Refs. 7, 8 to be more than 8 K. On the other hand, the positive thermal expansion of pure fullerite at $T < 2$ K implies the presence of processes other than two-well tunneling (probably, the conventional phonon mechanism is still valid) at this low temperature.

The possibility of detecting experimentally the negative contribution to thermal expansion due to the tunneling objects depends strongly on the relative magnitude of the positive (conventional) and negative (tunneling in this case) contributions. In the case of fullerite, the negative contribution is more pronounced, but one still encounters difficulty in determining the tunneling object. The first hypothesis of a tunneling of regular C_{60} molecules between P and H orientations [14] had the drawback of a high interwell potential barrier. The subsequent introduction of the idea of a competition of the isotropic and anisotropic parts of intermolecular interaction potential (though in orientational glass) [25] has lead to the current understanding (given in our previous paper [15] and the present one) that the tunneling objects are strongly localized orientational defects of the fullerite structure. A more detailed description of such defects could be obtained with the help of a more realistic three-dimensional modeling of the C_{60} crystal structure, which should be a subject for future studies.

Acknowledgments

We would like to thank Profs. A.S. Bakai, Yu.B. Gaididei, M.A. Ivanov, and V.G. Manzhelii, as well as Dr. A.N. Alexandrovskii for valuable and critical discussions. This study was supported in part by the Program «Investigation of Fundamental Problems and Properties of the Matter on Micro- and Macrolevels» of the National Academy of Sciences of Ukraine, by the INTAS Foundation under Grant INTAS 97-0368, and also by project No. 2669 «Structure and plasticity of fullerite» of Science Technology Center of Ukraine.

* For the case of ferromagnets the domain wall width is of the order of $a\sqrt{J/A}$, where a is the lattice spacing, J is the exchange, and A is the anisotropy. Since A is a relativistic correction, the ratio J/A can be increased up to 10^6. But for the present case of one interaction this ratio is about 1.

1. V.M. Loktev, *Fiz. Nizk. Temp*. **18**, 217 (1992) [*Low Temp. Phys*. **18**, 149 (1992)].
2. A.P. Ramirez, *Condens. Matter News* **3**, 6 (1994).
3. O. Gunnarsson, *Rev. Mod. Phys*. **69**, 575 (1997).
4. H. Kuzmany, B. Burger, and J. Kurty, in: *Optical and Electronic Properties of Fullerenes and Fullerene-based Materials*, J. Shinar, Z.V. Vardeny, and Z.H. Kaffafi (eds.), Marsel Dekker, New York (2000).
5. V.B. Efimov, L.P. Mezhov-Deglin, and R.K. Nikolaev, *JETP Lett*. **65**, 687 (1997).
6. V.B. Efimov and L.P. Mezhov-Deglin, *Physica* **B263–264**, 705 (1999).
7. A.N. Aleksandrovskii, V.B. Esel'son, V.G. Manzhelii, A.V. Soldatov, B. Sundqvist, and B.G. Udovidchenko, *Fiz. Nizk. Temp*. **23**, 1256 (1997) [*Low Temp. Phys*. **23**, 943 (1997)]; *ibid*. **26**, 100 (2000) [**26**, 75 (2000)].
8. A.N. Aleksandrovskii, V.G. Gavrilko, V.B. Esel'son, V.G. Manzhelii, B. Sundqvist, B.G. Udovidchenko, and V.P. Maletskiy, *Fiz. Nizk. Temp*. **27**, 333 (2001) [*Low Temp. Phys*. **27**, 245 (2001)]; *ibid*. **27**, 1401 (2001) [**27**, 1033 (2001)].
9. J.P. Olson, K.A. Topp, and R.O. Pohl, *Science* **259**, 1145 (1993).
10. R.C. Yu, N. Tea, M.B. Salamon, D. Lorents, and R. Malhotra, *Phys. Rev. Lett*. **23**, 2050 (1992).
11. S. Savin, A.B. Harris, and T. Yildirim, *Phys. Rev*. **B55**, 14182 (1997).
12. M. David, R. Ibberson, T. Dennis, and K. Prassides, *Europhys. Lett*. **18**, 219 (1992).
13. S.P. Tewari, P. Silotia, and K. Bera, *Solid State Commun*. **107**, 129 (1998).
14. M.A. Ivanov and V.M. Loktev, *Fiz. Nizk. Temp*. **19**, 618 (1993) [*Low Temp. Phys*. **19**, 442 (1993)].
15. V.M. Loktev, Yu.G. Pogorelov, and Ju.M. Khalack, *Fiz. Nizk. Temp*. **27**, 539 (2001) [*Low Temp. Phys*. **27**, 397 (2001)].
16. P. Launois, S. Ravy, and R. Moret, *Phys. Rev*. **B55**, 2651 (1997).
17. V.M. Loktev, *Fiz. Nizk. Temp*. **5**, 295 (1979) [*Sov. J. Low Temp. Phys*. **5**, 142 (1979)].
18. H. Wang, C. Zeng, B. Wang, J.G. Hou, Q. Li, and J. Yang, *Phys. Rev*. **B63**, 085417 (2001).
19. G. Van Tendeloo, S. Amelinckx, M.A. Verheijen, P.H.M. van Loosdrecht, and G. Meijer, *Phys. Rev. Lett.* **69**, 1065 (1992).
20. E.J.J. Groenen, O.G. Poluektov, M. Matsushita, J. Schmidt, J.H. van der Waals, and G. Meijer, *Chem. Phys. Lett*. **197**, 314 (1992).
21. C. Laforge, D. Passerone, A.B. Harris, P. Lambin, and E. Tosatti, *Phys. Rev. Lett*. **87**, 085503 (2001).
22. J.G. Hou, J. Yang, H. Wang, Q. Li, C. Zeng, I. Yuan, B. Wang, D.M. Chen, and Q. Zhu, *Nature* **409**, 304 (2001).
23. T. Vegge, J.P. Sethna, S.A. Cheong, K.W. Jacobsen, C.R. Myers, and D.C. Ralph, *Phys. Rev. Lett*. **86**, 1546 (2001).
24. Yu.A. Freiman, *Fiz. Nizk. Temp*. **9**, 657 (1983) [*Sov. J. Low Temp. Phys*. **9**, 335 (1983)].
25. V.M. Loktev, *Fiz. Nizk. Temp*. **25**, 1099 (1999) [*Low Temp. Phys*. **25**, 823 (1999)].